Dynamics of a solar sail around an asteroid

Iain Moore* and Matteo Ceriotti†
University of Glasgow, Glasgow, Scotland, G12 8QQ, United Kingdom.

Abstract

Asteroids pose both a threat and an opportunity: the threat of a catastrophic collision, the opportunity to learn about the early solar system from these pristine relics, and the possibility of exploiting their wealth of raw materials. A critical element of any mission study is in the orbital dynamics for trajectory planning. Using the Augmented Hills Restricted 3-Body Problem (AH3BP), several orbit options were sought around asteroids 2000 SG_{344} and 2008 EV_5 for a solar sail spacecraft. Initial orbits were obtained for a spacecraft without the added acceleration of the sail. These were then used as initial conditions for increasing sail performance. Under the weak gravitational attraction of such small asteroids, the Solar Radiation Pressure (SRP) proved overpowering and periodic orbits were not possible. Methods of sail performance reduction were investigated with the aim of reducing the performance to such a point as to permit periodic orbits. The final orbits were then selected and possible transfer trajectories to the asteroid, from the interplanetary phase of the mission, were established using invariant manifolds.

1 Introduction

Since the discovery of Ceres in 1801, asteroids have filled the imagination of astronomers. In more recent times, asteroids have come to represent both a threat and an opportunity. The proximity of Near-Earth Asteroids (NEAs) to the Earth, and the tendency of some to cross the orbit of the Earth, could have serious consequences for the delicate balance of life on this planet. However, this proximity to the Earth also makes them attractive candidates for exploration. In addition, their wealth of raw minerals makes them excellent candidates for the resource mining which will provide much of the infrastructure for the colonisation of the solar system by humanity as it pushes out into the final frontier [1]. With all of the intrigue surrounding asteroids, and the accessibility of NEAs, it was inevitable that humanity would find its way to these ancient wanderers. Thus far, there been several missions to asteroids: the NEAR-Shoemaker mission to asteroid 433 Eros [2], the Hayabusa mission to asteroid Itokawa [3], and NASAs Dawn mission to Vesta and Ceres [4]. More recently, the Japanese Aerospace Exploration Agency (JAXA) completed the second of their Hayabusa missions with Hayabusa 2 which made the first successful landings of spacecraft on an asteroid with the MASCOT landers. In September 2016, NASA launched its latest NEA mission to asteroid Bennu where the primary objective is that of a sample return to the Earth [5]. On December 31st, 2018, the OSIRIS-REx spacecraft entered a closed orbit around asteroid Bennu, breaking the record for the smallest body around which a spacecraft has ever orbited. And future missions are abound: there is the NASA NEA Scout [6] mission which proposes to visit a NEA using a solar sail as the primary propulsion system, the ESA Asteroid Impact Mission (AIM), and NASAs Double Asteroid Redirection Test. The last two missions are actually two-parts of the larger Asteroid Impact and Diversion Assessment (AIDA) mission which plans to assess the effects of an impacting spacecraft on an asteroid and how this impact affects the asteroid orbit.

There have been numerous studies of the dynamics of a solar sail in the vicinity of an asteroid [7][8][9][10]. Farrés *et al* [7][8] take a detailed look in the restricted 3-body problem. The effect of a solar sail, which remains perpendicular to the Sun-sail line, is to push the L_1 equilibrium point further from the asteroid in the direction of the Sun. This brings limitations in its use of proximity operations at the asteroid and so [7] and [8] provide orbital options from L_2 which allow for some of the orbital period to extend into the sunlit side of the asteroid: an important consideration for observational missions. Morrow *et al* [9] again implement a restricted 3-body problem to study orbits around asteroid Vesta. They also consider the effect of the sail performance for orbiting smaller bodies and conclude that there is a limit in performance of sail for which periodic

*PhD Candidate (Space Systems Engineering), School of Engineering, Room 612 James Watt Building (South), University of Glasgow, Glasgow, Scotland, G12 8QQ, United Kingdom. i.moore.3@research.gla.ac.uk

†Lecturer (Space Systems Engineering), School of Engineering, Room 625 James Watt Building (South), University of Glasgow, Glasgow, Scotland, G12 8QQ, United Kingdom. matteo.ceriotti@glasgow.ac.uk

orbits are possible for any given asteroid. This presents a problem for sails in proximity of very small asteroids such as those of [11] which form the focus of this work.

Peloni *et al* [11] have produced an optimised trajectory for a solar sail spacecraft to visit 5 NEAs in a period of less than 10 years. This work shows the exciting possibilities opened up by solar sail technology to deliver high energy missions. Table 1 shows the five asteroids in the optimised sequence of this work with orbital and physical paramenters shown for each asteroid.

Table 1: Properties of the encounters of the considered sequence (taken from Peloni *et al* [11])

Object	2000 SG_{344}	2015 JD_3	2012 KB_4	2008 EV_5	2014 MP
Orbit Type	Aten	Amor	Amor	Aten	Amor
Semi-major Axis (AU)	0.977	1.058	1.093	0.958	1.050
Eccentricity	0.067	0.009	0.061	0.083	0.029
Inclination (deg)	0.111	2.730	6.328	7.437	9.563
Absolute Magnitude (mag)	24.7	25.6	25.3	20	26
Estimated size (m)	$35-75$	$20-50$	$20-50$	$260-590$	$17-37$
Inclination (deg)	0.111	2.730	6.328	7.437	9.563
EMOID (AU)	0.0008	0.054	0.073	0.014	0.020
PHA	no	no	no	yes	no
NHATS	yes	yes	yes	yes	yes

This project is an extension of this mission where the proximity orbits near asteroids 2000 SG_{344} and 2008 EV_5 will be examined. Furthering the understanding of the dynamical environment in proximity asteroids will provide crucial tools to mission planners of future asteroid missions

In section 2, solar sails and the 3-body problem are introduced before the particular variation of the restricted 3-body problem used in this work is defined. The numerical method of searching for periodic orbits is then discussed. In section 3 the results for various orbit types and varying sail performance are presented. Section 4 then presents results for orbits at asteroid 2008 EV_5. Following this, section 5 discusses methods to reduce the sail performance before the transfers using invariant manifolds are presented in section 6.

2 Solar Sails and the 3-Body Problem

Solar sails are a particular form of low-thrust propulsion system that require no on-board propellant to function. The sail is a large, thin, and highly reflective membrane which operates by reflecting photons radiated by the Sun. The first component of force comes from the incident photons, $\mathbf{u}_i$, which impart their momentum upon impact with the sail. A second component of force is that imparted by the reflected photons, $\mathbf{u}_r$. These components then give the total force vector, as shown in Fig. 1a.

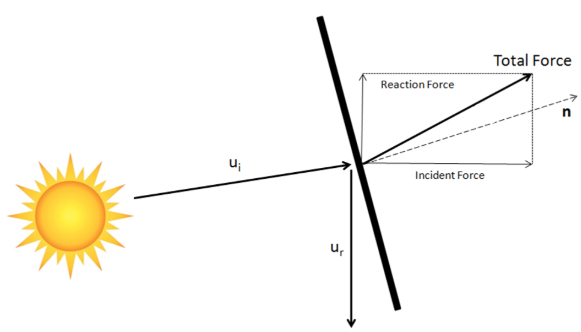

(a) Diagram of solar sail force model

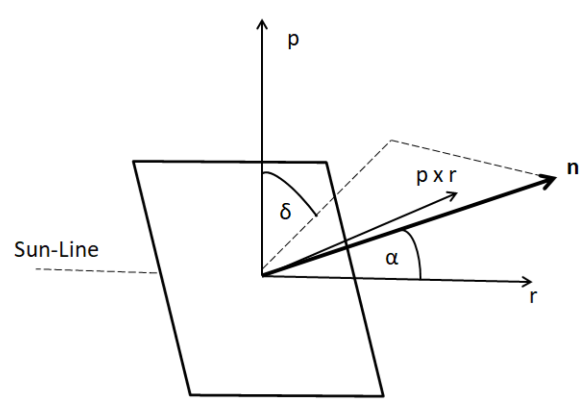

(b) Diagram showing sail orientation via cone and clock angles (taken from [22])

Figure 1

The sail orientation is defined by the so-called cone and clock angles, α and δ respectively. These angles are shown in Fig. 1b where vector $\mathbf{n}$ is the vector normal to the sail surface (the sail normal), $\mathbf{r}$ is a vector in the direction of the Sun-line and $\mathbf{p}$

is a vector in the direction normal to the orbital plane.

This work will consider the dynamics of a solar sail under the gravitational effects of both the Sun and the asteroid. These two larger bodies constitute the primaries of the Restricted 3-Body Problem (R3BP) [12]. This is an approximation of the full 3-body problem where one of the bodies, in our case the spacecraft (our secondary body), is of negligible mass compared with the larger bodies. With negligible mass, the spacecraft will be considered to have no effect on the two primary bodies.

A variation of the restricted 3-body problem will be used which accounts for the vanishingly small mass of the asteroid in comparison with the sun. This model, referred to as the Augmented Hills 3-Body Problem (AH3BP) [8], centres the reference frame on the asteroid (Fig. 2) while accounting for the very small mass ratio of the system. The mass ratio is the ratio of the smaller primary (the asteroid) to the total mass of the Sun-asteroid system.

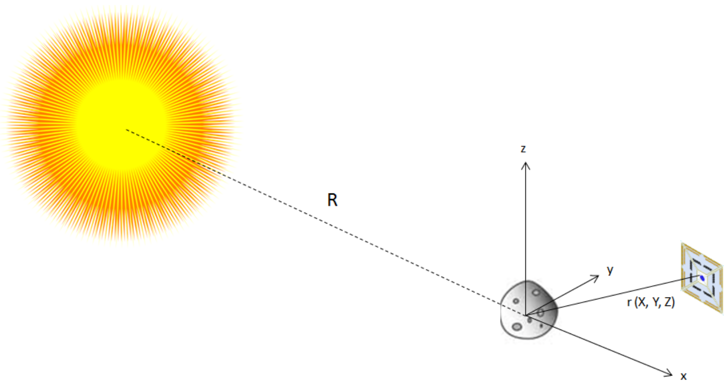

Figure 2: Sun-Asteroid Synodic Reference Frame Centred on the Asteroid

The equations of motion for the AH3BP are given in [7] and [8]:

$$
\begin{aligned}
\ddot{x} - 2\dot{y} &= \frac{\partial \Omega}{\partial x} + a_x \\
\ddot{y} + 2\dot{x} &= \frac{\partial \Omega}{\partial y} + a_y \\
\ddot{z} &= \frac{\partial \Omega}{\partial z} + a_z
\end{aligned}
\tag{2.1}
$$

where

$$\Omega(x, y, z) = \frac{1}{r} + \frac{1}{2}(3x^2 - z^2)$$

(x, y, z) denotes the position of the solar sail in the frame rotating with the asteroid's orbit around the Sun, and $r = \sqrt{x^2 + y^2 + z^2}$. The remaining terms in equations 2.1 are the partial derivatives, and the acceleration terms $\mathbf{a}_{sail} = (a_x, a_y, a_z)$. The acceleration terms are then given in component form as [7]:

$$
\begin{aligned}
a_x &= \overline{\beta}(\rho \cos^3 \alpha \cos^3 \delta + 0.5(1 - \rho) \cos \alpha \cos \delta) \\
a_y &= \overline{\beta}(\rho \cos^2 \alpha \cos^3 \delta \sin \alpha) \\
a_z &= \overline{\beta}(\rho \cos^2 \alpha \cos^2 \delta \sin \delta)
\end{aligned}
\tag{2.2}
$$

where $\overline{\beta} = \beta(\mu_{sb}\omega^4)$ and ρ is the sail reflectivity ($\rho = 1$ for a perfect reflector), and $\mu_{sb} = GM_{sb}$ with G being the universal gravitational constant and M_{sb} the mass of the asteroid. This now leaves the partial derivative terms to be expanded:

$$
\begin{aligned}
\frac{\partial \Omega}{\partial x} &= x\left(3 - r^3\right) \\
\frac{\partial \Omega}{\partial y} &= -yr^3 \\
\frac{\partial \Omega}{\partial z} &= -z\left(r^3 + 1\right)
\end{aligned}
\tag{2.3}
$$

Now, substituting equations 2.2 and 2.3 into 2.1, we have the final equations of motion in terms of the known parameters:

$$
\begin{aligned}
\ddot{x} &= 2\dot{y} + x\left(3 - r^3\right) + \overline{\beta}(\rho\cos^3\alpha\cos^3\delta + 0.5(1-\rho)\cos\alpha\cos\delta) \\
\ddot{y} &= -2\dot{x} - yr^3 + \overline{\beta}(\rho\cos^2\alpha\cos^3\delta\sin\alpha) \\
\ddot{z} &= -z\left(r^3 + 1\right) + \overline{\beta}(\rho\cos^2\alpha\cos^2\delta\sin\delta)
\end{aligned}
\tag{2.4}
$$

The AH3BP system also admits an integral of motion which gives rise to a constant of integration, called the Jacobi constant:

$$
J_c = \dot{x}^2 + \dot{y}^2 + \dot{z}^2 - 2\Omega(x, y, z) + a_x x + a_y y + a_z z \tag{2.5}
$$

As the work of Peloni *et al* [11] requires use of the performance parameter characteristic acceleration (a_c), a conversion is required from a_c to $\overline{\beta}$. This conversion is given in equation 2.6:

$$
\overline{\beta} = \frac{K_1 a_c}{2\rho P_0\left(\frac{r_0}{r}\right)^2 \mu_{sb}^{\frac{1}{3}}} \tag{2.6}
$$

where r_0 is the mean radius of the asteroid and K_1 is a constant.

With the dynamics of the system established, it is now necessary to establish a set of initial conditions to pass to the numerical integration and continuation methods. Given that these initial conditions are in a 6-dimensional state space:

$$
\mathbf{s}_0 = (x_0, y_0, z_0, \dot{x}_0, \dot{y}_0, \dot{z}_0)
$$

it is convenient to reduce the number of terms. Gurfil *et al* [13] provide a useful method of reducing the number of required variables. First, by considering a planar orbit, two terms can be removed. For an orbit in the x-y plane, $z = \dot{z} = 0$:

$$
\mathbf{s}_0 = (x_0, y_0, 0, \dot{x}_0, \dot{y}_0, 0)
$$

Then, by considering only orbits which are symmetrical around x, it must be that the orbit intersects the x-axis. Thus, we can set the initial condition of $y_0 = 0$:

$$
\mathbf{s}_0 = (x_0, 0, 0, \dot{x}_0, \dot{y}_0, 0)
$$

This symmetry will also guarantee that the initial velocity is in the y-direction only, so $\dot{x}_0 = 0$:

$$
\mathbf{s}_0 = (x_0, 0, 0, 0, \dot{y}_0, 0)
$$

Therefore, all that is required now is to find x_0 and $\dot{y}_0$. It is also convenient to use the Jacobi integral in search of $\dot{y}_0$. The Jacobi integral, given in equation 2.5, then reduces to:

$$
J_c = \dot{y}_0^2 - \frac{2}{x_0} - 3x_0^2 + a_{x_0} x_0 \tag{2.7}
$$

By choosing a value for J_c and x_0, equation 2.7 yields the final variable, $\dot{y}_0$. With this initial guess, a suitable numerical method can be used to adjust the values of x_0 and J_c until a periodic orbit is found [13]. Where $z_0 \neq 0$, the Jacobi constant is given by:

$$
J_c = \dot{y}_0^2 - \frac{2}{\sqrt{x_0^2 + z_0^2}} - \left(3x_0^2 - z_0^2\right) + a_{x_0} x_0 + a_{z_0} z_0 \tag{2.8}
$$

3 Periodic orbits at Asteroid 2000 SG_{344}

Initially, orbits were obtained for a value of $\overline{\beta} = 0$ (sail fully stowed) so as to obtain initial conditions which could later be used in the search of periodic orbits when applying $\overline{\beta} \neq 0$ (sail deployed).

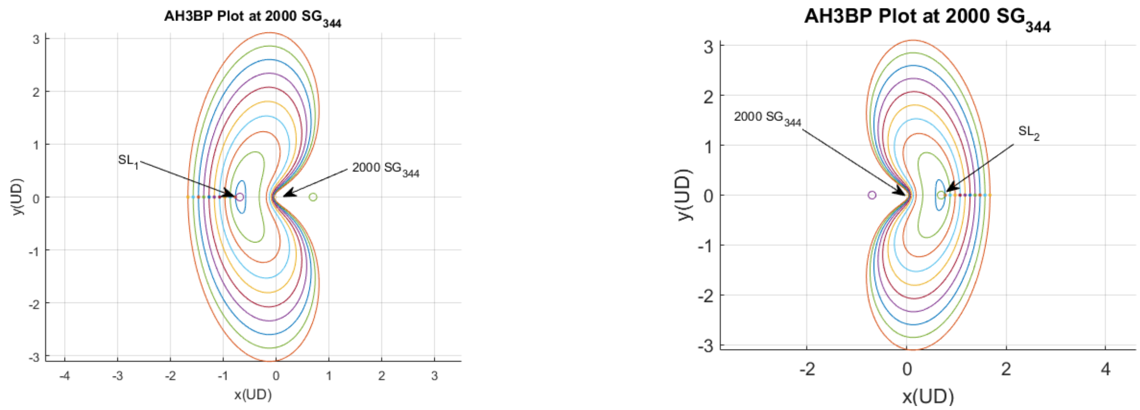

(a) SL_1 (b) SL_2

Figure 3: Family of Planar Lyapunov orbits

3.1 Periodic Orbits for $\overline{\beta} = 0$

Periodic orbits, quasi-periodic orbits, and equilibrium points are all special solutions of the three body problem [14].

The equilibrium points themselves contain a 1-dimensional stable and unstable manifold, as well as a 4-dimensional centre manifold. Within the centre manifold are two types of periodic motion: an in-plane periodic orbit, also known as a Lyapunov orbit; the second is an out of plane, almost vertical orbit [14]. The planar Lyapunov orbits around equilibrium points SL_1 and SL_2 are shown in figure 3.

Another type of periodic motion is the Halo orbit. As the amplitude of the orbit along the family of Lyapunov orbits increases, there comes a point at which the family reaches a critical amplitude. At this point, a bifurcation occurs [14], from which the Halo family is born. In order to establish at which point they bifurcate, it is necessary to do a study of the bifurcation points. Such a detailed study can be found in [16]. In the AH3BP system, the planar Lyapunov orbit at this bifurcation point was found to have initial condition $\mathbf{s}_0 = (-0.7747, 0, 0, 0, 0.6138, 0)$, a maximum y-amplitude of 0.3082 UD, and is shown, continued into the family of southern Halo orbits to which it bifurcates, in figure 4. These Halo orbits are referred to as "southern" because they continue out from below the plane. There are also northern Halo orbits which extend out and above the plane.

The Halo orbits, bifurcated from the Lyapunov orbits around equilibrium point SL_1, are shown with increasing amplitude in figure 4. A similar set of Halo orbits are also found after their bifurcation from the Lyapunov orbits around SL_2.

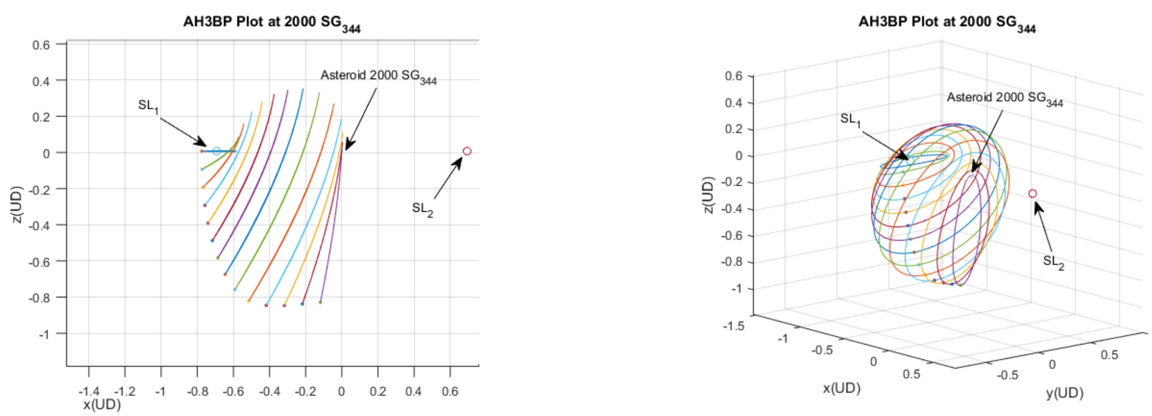

(a) (b)

Figure 4: Lyapunov to Southern Halo Orbit Bifurcation

After this first bifurcation, again following the planar Lyapunov orbits of increasing amplitude, the next bifurcation is reached. This bifurcation is from planar Lyapunov to Axial orbit.

Beyond the equilibrium point orbits, motion around the asteroid itself was also investigated. In order to achieve stable orbits, it would be preferable to see those orbits from the f family, as described in [13]. Figure 5a shows this family, the plot matching very well with those of Gurfil *et al* (2016).

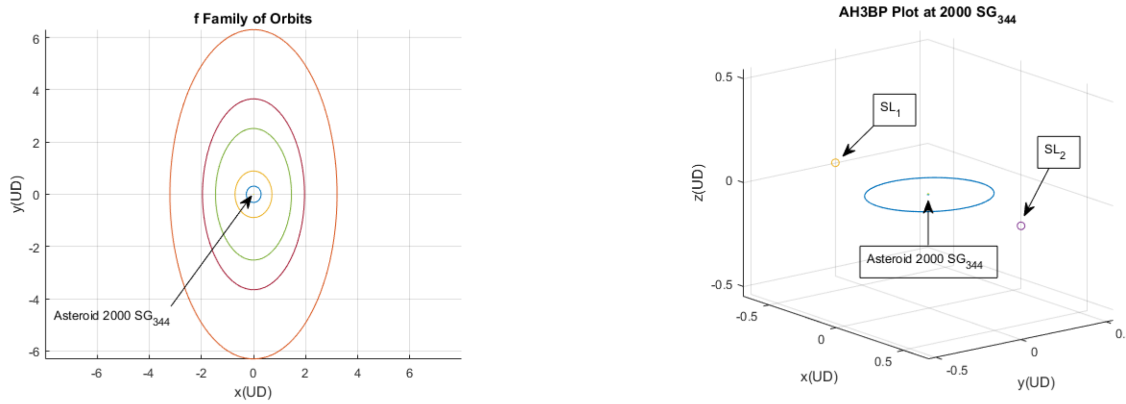

(a) f family of orbits (b) Circular Orbit of the f Family

Figure 5: Orbits from the f family

From this family, a given level of energy will lead to different orbits being achieved. Figure 5b shows an orbit for $J_c = -4.5031$.

3.2 Periodic Orbits for $\overline{\beta} \neq 0$

Not only do we find the forces on the sail due to SRP can be greater than those felt by the gravitational field of the asteroid, but also the equilibrium points will be displaced according to the value of $\overline{\beta}$ as well as the sail orientation in α and δ [8]. As the lightness number is normalised with respect to the small body which is being orbited, the smaller the body, the larger the value of $\overline{\beta}$, as shown in equation 2.6. With increasing $\overline{\beta}$, [7] and [8] show that the SL_1 point is moved away from the small body in the Sun direction. For very large $\overline{\beta}$, this distance becomes very limiting for the use of orbits around that equilibrium point.

For asteroid 2000 SG_{344}, taking an acceptable characteristic acceleration to permit orbital operations of $a_c = 0.0001$ mm/s^2 (giving $\overline{\beta} = 3576.5$), the equilibrium points are moved to $SL_1 = (-149.020866552956, 0, 0)$ and $SL_2 = (0.0472875656945215, 0, 0)$. Therefore, the SL_1 point, and its associated Lyapunov orbits, become unusable at such length scales.

Farrés *et al* [7] states that most of the periodic motion around an asteroid for a solar sail is contained on the dark side of the asteroid. However, there are some periodic orbits which spend up to 50% of their time in the sun-lit side, and so these orbits will be pursued in the next phase of this work.

3.2.1 Planar Lyapunov Orbits around SL_2

Taking the initial conditions for a planar Lyapunov orbit around SL_2, such as those shown in figure 3, we gradually increase the value of $\overline{\beta}$. This iterative approach was successful up to a point at which the same issue arose where the software simply cannot converge to a solution. This point, which represents the divergence from periodic solutions, occurs at $\overline{\beta} = 120.8947$. The value of $\overline{\beta} = 120.8947$ represents a characteristic acceleration value of $a_c = 2.7042 \times 10^{-8}$ mm/s^2. Given that the target characteristic acceleration, in order to match the work of Peloni *et al*, is $a_c = 0.2$ mm/s^2, the value of $a_c = 2.7042 \times 10^{-8}$ mm/s^2 proves too restrictive to be considered feasible. Therefore, this work concludes that, for a small asteroid of 37 m diameter, there are no periodic solutions in the planar Lyapunov family for a solar sail spacecraft. In order to use such orbits, the solar sail would need to be “switched off”.

4 Periodic orbits at Asteroid 2008 EV_5

With the conclusion that periodic orbits with a solar sail about asteroid 2000 SG_{344} are not possible, progress along the target asteroids of the work by Peloni *et al* [11] presented an opportunity to attempt orbital operations around a larger body, asteroid 2008 EV_5. With a mass of 1×10^{11} kg [17], this asteroid provided the possibility of a solar sail of up to $a_c = 0.00957$ mm/s^2 [9].

Similar problems were encountered as those for asteroid 2000 SG_{344}, where the introduction of non-zero values of $\overline{\beta}$ quickly led to a divergence from periodic solutions. There was also a similar rapid displacement of the equilibrium points.

These issues were tested with the application of gradually increasing values of of $\overline{\beta}$ for a range of different orbit types. These orbits were: circular orbits around the asteroid, planar Lyapunov orbits around SL_2, and Halo orbits around SL_2. The subsequent section details the results and analysis for the simulations of each type of orbit.

For planar circular orbits around the asteroid, this divergence was immediate which meant that, in this work, the orbits were not feasible with the introduction of a solar sail. In order to facilitate such an orbit, further work would be required to investigate techniques which would allow such an orbit. These may include, but are not limited to, solar sail steering laws and sail performance variation.

Planar Lyapunov orbits around libration point SL_2 presented some more interesting results. Having begun from the planar Lyapunov bifurcation orbit, the solar sail causes the initially bifurcating orbits to have smaller amplitudes compared to those of Fig. 4 before the amplitudes grow again. Fig. 6 shows the continuation along the value of $\overline{\beta}$, starting from the critical planar Lyapunov orbit which bifurcates into Halo orbits of increasing energy.

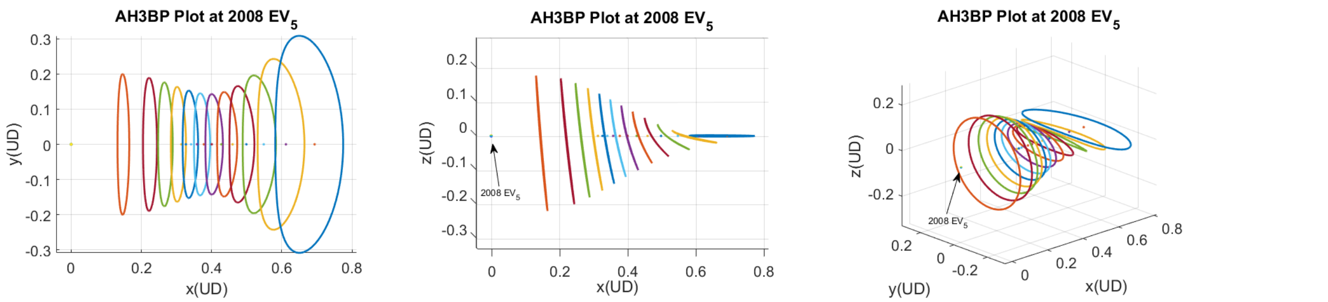

(a) x-y plane (b) x-z plane (c) Isometric View

Figure 6: Bifurcation of Lyapunov to Halo orbits under SRP perturbation

Although the results are interesting, the problem remains that these orbits are for very small values of $\overline{\beta}$. With the closest orbit to the asteroid in Fig. 6 having a value of $\overline{\beta} = 9.287693$ ($a_c = 0.00002$ mm/s^2). Beyond these values, periodic orbits cannot be found.

Halo orbits were then tested to see if there were any possible periodic orbits for sufficiently high values of $\overline{\beta}$. Fig. 7 shows the results for such a test beginning from a mid-range halo orbit.

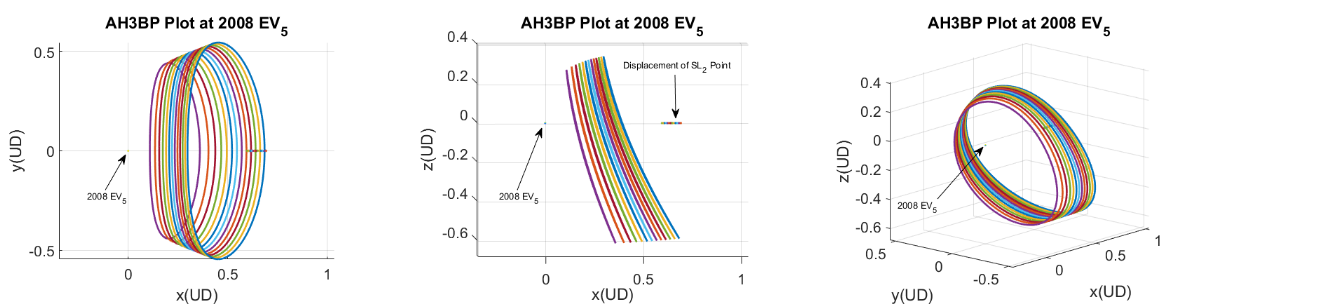

(a) x-y plane (b) x-z plane (c) Isometric View

Figure 7: Halo orbits around SL_2 under SRP perturbation

The orbits are displaced towards the asteroid by the SRP force, along with the displacement of the SL_2 point towards the asteroid. However, the simulation once again breaks down for very small values of a_c and $\overline{\beta}$. In this case, the orbit closest to the asteroid represents $\overline{\beta} = 1.073431$ ($a_c = 0.000003$ mm/s^2).

The difficulties encountered have given encouragement to investigate novel methods to vary the performance of the solar sail. Particularly, the ability to "switch off" the sail would be very beneficial for this work.

5 Reducing the Solar Sail Performance to Permit Orbital Operations

Asteroids on the order of tens of metres have such a weak gravitational pull that the force felt from the SRP is often overpowering and there is simply no feasible bound orbit around the asteroid. From [9], the level of acceptable sail performance for a range of asteroid radii are shown in Fig. 8 for the 3 main types of asteroid [18] based on their average densities [19]. The overall average density is also plotted as fully accurate compositions cannot be obtained from Earth-based observation alone, and so it is this average density that is used when estimating the mass of a body in this work.

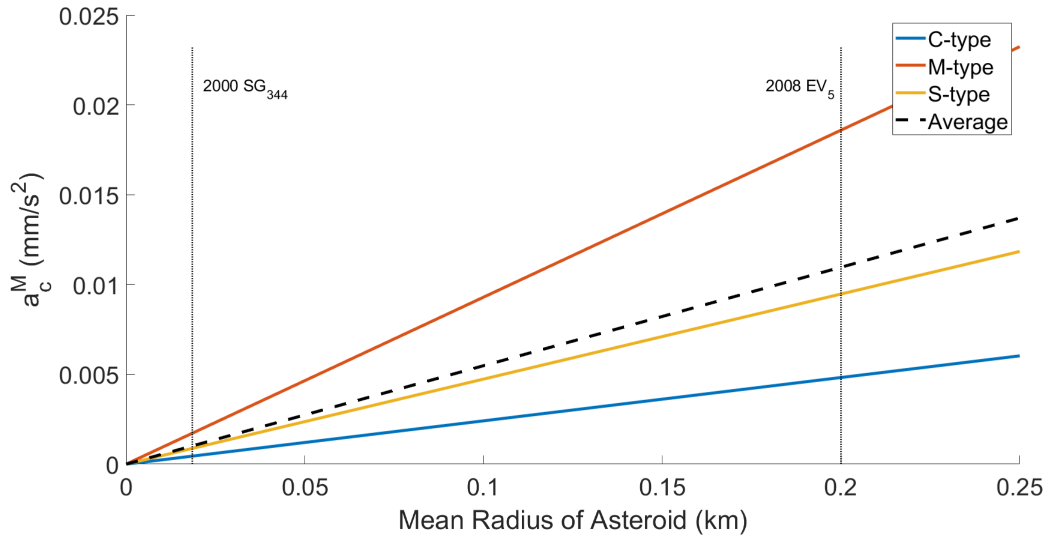

Figure 8: The range of a_c^M for changing asteroid radius

Fig. 8 shows that, for the very small bodies considered in this work, the maximum permissible value of a_c is orders of magnitude lower than the sail of Peloni *et al* [11].

There are several methods given in the literature for reducing the overall performance of a solar sail. Such methods become critical to a situation where orbital operations around a very small body are required. In this work, proximity operations around asteroids 2000 SG_{344} and 2008 EV_5 have shown that, for a solar sail, periodic orbital operations would not be feasible. However, the overall mission of prospecting multiple asteroids would still benefit greatly from use of a solar sail in the interplanetary phase. Therefore, where the mission takes the spacecraft to a small bodies such as 2000 SG_{344} and 2008 EV_5, it would be useful to have the ability to remove the accelerations due to the solar sail. With this ability, the spacecraft would have access to all of the $\overline{\beta} = 0$ orbits of section 3.1.

In [20] and [21] a concept is presented to vary the reflectivity of the sail to allow control over the sail orientation. It would be possible (as shown in Fig. 9) to apply this variation evenly to simply reduce the effective are of the sail. However, there are two-components of force provided to the sail by photons radiated by the Sun [22]. The component imparted by incident photons and that by reflected photons. So, although this method can remove the effect of the reflected photons, it does not reduce the effect of incident photons. Therefore, the maximum performance reduction is only 50%, a far lower reduction than that which is required here.

May-Wilson [23] presents a method of reducing the sail performance by constantly changing the sail orientation so as to average out a smaller performance value. However, this work again found a limitation to a reduction of 50%.

Williams and Abate [10] present a possible solution in the form of a furlable sail. This would allow the sail to be extended and retracted as required. With the sail fully stowed, the mission would have access to all of the orbits for $\overline{\beta} = 0$. However, one of the great challenges in practical solar sailing is in the deployment of the sail. As such, with current technology, the furlable sail would present a high risk to mission success. Though a high risk, it is the only available option which presents the possibility of complete sail performance reduction.

6 Transfer to and from the Periodic Orbits

For the orbits of $\overline{\beta} = 0$, it is necessary to find potential entry points into these orbits which would allow the capture of the spacecraft by the asteroid at arrival, as well as the escape from the asteroid upon departure. In order to establish these insertion and escape trajectories, it was necessary to choose one orbit, from the family of orbits, on which to concentrate. The study will now focus only on asteroid 2008 EV_5 and figures will now show dimensional units for appreciation of proximity to the asteroid.

There were two main type of orbit investigated, those being the planar Lyapunov and Halo orbits. The optimal orbit, for scientific purposes, would be continually on the sun-lit side of the asteroid and would be within sufficient distance for the onboard observation instruments to be effective. Fig. 11 show the different orbits and their associated variation of distance

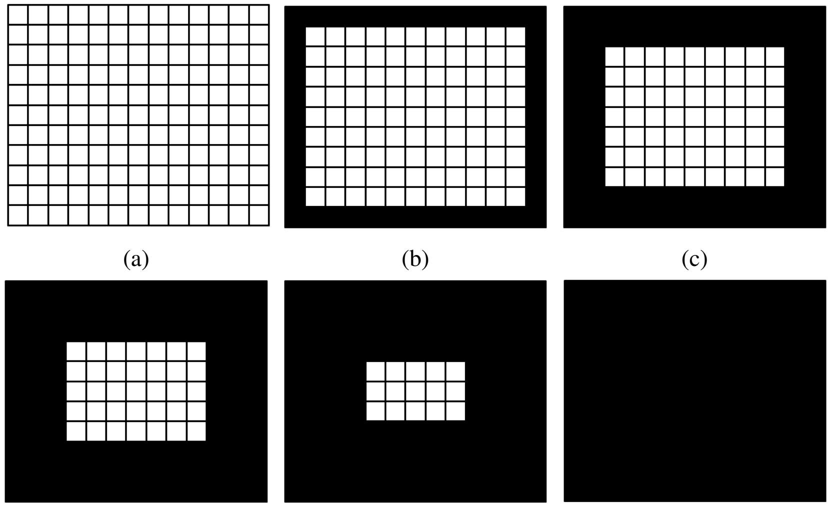

(a) (b) (c)

(d) (e) (f)

Figure 9: Changing reflectivity under $\overline{\beta}$-control

over the period of that orbit. The colour coding of the orbit plots is consistent with the colour coding of the distance plots. In order to maintain the spacecraft orbit on the sun-lit side of the asteroid, orbits around equilibrium point SL_1 are the obvious choice.

For asteroid 2008 EV_5, the choice of orbit comes with the complication that the equilibrium points are now approximately 35 km from the asteroid and so it is necessary to bring at least some of the orbit much closer. Fig. 10 gives the orbit plots and distance from asteroid plots for the planar Lyapunov family of orbits.

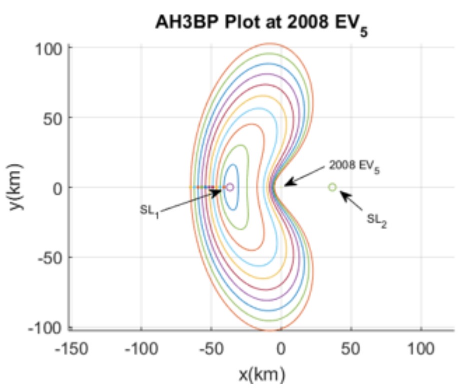

(a) Orbits

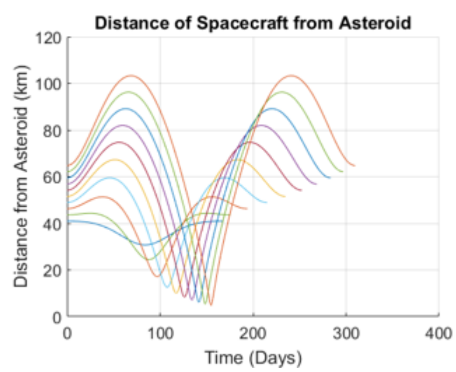

(b) Distances of orbits from asteroid

Figure 10: Plot of orbits and distances for planar Lyapunov orbits about SL_1 at asteroid 2008 EV_5

By choosing the highest amplitude orbit, the spacecraft can be brought to within 5 km of the asteroid at the closest pass. However, the spacecraft would spend a large part of the orbit either too far for effective observation or on the dark side of the asteroid. Therefore, over the full orbital period of 309.6 days, the optimal observational time would be the 6.16 days when the spacecraft re-enters the sun-lit side, within close proximity, of the asteroid. This observational period would take the spacecraft from 10 km distance from the asteroid it initiation, to 5 km from the asteroid at closest pass.

For 2008 EV_5, the halo orbits bring far greater benefits. For a small penalty in maximum distance compared to the planar option, the orbit indicated in Fig. 11a brings the orbit within the 10 km range for a period similar to that of the high amplitude planar Lyapunov orbit, in this case 6.64 days. However, the period of this orbit is just 90.27 days. Therefore, the spacecraft will be able to make 3.43 passes for every pass of the spacecraft on the planar Lyapunov orbit. This would also allow this work to maintain the prescribed itinerary of the work of Peloni *et al* [11] where each proximity phase can last only a few months to allow the target mission duration to remain under 10 years.

Invariant manifolds [24] are used to provide possible insertion and escape trajectories from and to the interplanetary phase of the mission. These are shown in Fig. 12 to the halo orbit of Fig. 11.

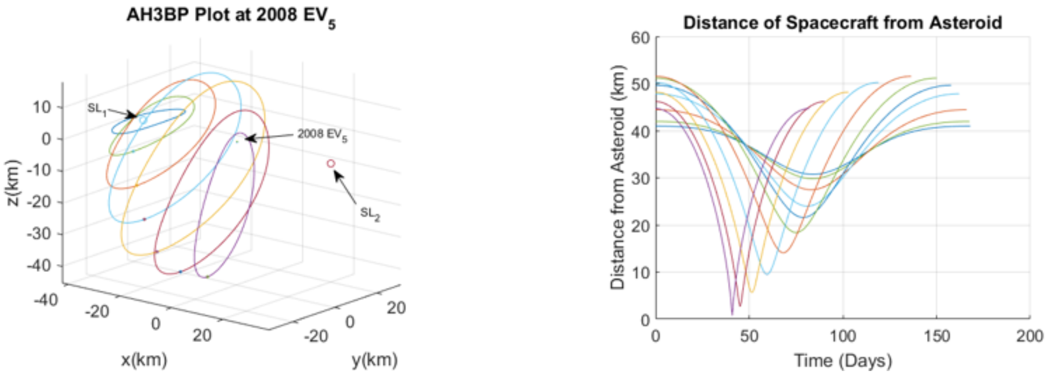

(a) Orbits (b) Distances of orbits from asteroid

Figure 11: Plot of orbits and distances for halo orbits about SL_1 at asteroid 2008 EV_5

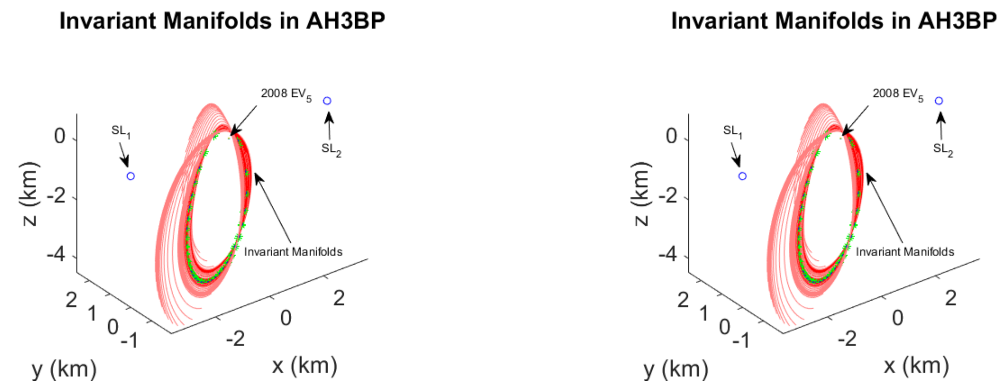

(a) Insertion (b) Escape

Figure 12: Plot of invariant manifolds allowing insertion and escape for halo orbits about SL_1 at asteroid 2008 EV_5

7 Conclusions

In this work, proximity orbits around asteroids 2000 SG_{344} and 2008 EV_5 from the work of Peloni *et al* [11] have been presented. Initially, the AH3BP model was described and implemented. Then, a method of searching for periodic orbits in this system, using a predictor-corrector method, was described. Using this method, periodic orbits were found for a value of $\overline{\beta} = 0$ for asteroids 2000 SG_{344} and 2008 EV_5. Once these were established, the value of $\overline{\beta}$ was gradually increased with the aim of finding periodic orbits with the solar sail fully deployed with the same performance of that in the work of Peloni *et al* [11].

Given the very weak gravitational pull of the asteroids considered in the work, the force applied to the spacecraft by the SRP was too overpowering even for very low values of $\overline{\beta}$. This meant that it was not possible to enter into bound periodic orbits around the asteroids with a solar sail of any meaningful size.

In order to alleviate these issues, methods of varying the reflectivity of the sail were presented. These methods included so-called $\overline{\beta}$-control, where the reflectivity of the sail could be varied. Another option was to use time-averaged performance reduction through changing the sail orientation. However, these performance reductions were limited to a 50% reduction only. Another method allowed for a furlable sail which could be stowed and deployed as required, allowing for complete reduction in sail performance, though with caveats regrading the current deployment technology.

With this reduction in performance, the spacecraft would have access to the previously established orbits for $\overline{\beta} = 0$.

Finally, transfer orbits into and out of the periodic orbits of $\overline{\beta} = 0$ were found using invariant manifold theory. These manifolds allow ballistic capture of the spacecraft by the asteroid upon arrival. Then, with a small perturbation, easy departure from the asteroid to re-join the interplanetary phase of the mission.

This work has shown that there are fascinating intricacies to orbiting very small bodies using solar sail spacecraft. The ability to vary the performance of the sail itself has been crucial in the success of the proximity operations.

References

[1] G. Genta and M. Rycroft, "Will space actually be the final frontier of humankind?," *Acta Astronautica*, vol. 58, no. 5, pp. 287–295, 2006.

[2] L. Prockter, S. Murchie, A. Cheng, A. Krimigis, R. Farquhar, A. Santo, and J. Trombka, "The near-shoemaker mission to asteroid 433 eros," *Acta Astronautica*, vol. 51, pp. 491 – 500, 2002.

[3] M. Yoshikawa, A. Fujiwara, and J. Kawaguchi, "Hayabusa and its adventure around the tiny asteroid itokawa," *Highlights of Astronomy*, vol. 14, pp. 323 – 324, 2006.

[4] D. J. Scheeres, *Orbital Motion in Strongly Perturbed Environments*. Springer-Praxis Books, 2012.

[5] S. G. Hesar, D. J. Scheeres, and J. W. McMahon, "Sensitivity analysis of the OSIRIS-REx terminator orbits to maneuver errors," *Journal of Guidance, Control, and Dynamics*, vol. 40, pp. 81 – 95, 2017.

[6] L. Johnson, J. Castillo-Rogez, J. Dervan, and L. McNutt, "Near earth asteroid (NEA) scout," in *International Symposium on Solar Sailing*, 2017.

[7] A. Farrés, A. Jorba, and J. Mondelo, "Orbital dynamics for a non-perfectly reflecting solar sail close to an asteroid," *2nd IAA Conference on Dynamics and Control of Space Systems*, 2014.

[8] A. Farrés, A. Jorba, and J. Mondelo, "Numerical study of the geometry of the phase space of the augmented hill three-body problem," *Celestial Mechanics and Dynamical Astronomy*, vol. 129, pp. 25–55, 2017.

[9] E. Morrow, D. J. Scheeres, and D. Lubin, "Solar sail orbit operations at asteroids," *Journal of Spacecraft and Rockets*, vol. 38, pp. 279–286, 2001.

[10] T. Williams and M. Abate, "Capabilities of furlable solar sails for asteroid proximity operations," *Journal of Spacecraft and Rockets*, vol. 46, pp. 967–975, 2009.

[11] A. Peloni, M. Ceriotti, and B. Dachwald, "Solar sail trajectory design for a multiple near-earth asteroid rendezvous mission.," *Journal of Guidance, Control, and Dynamics*, vol. 39, pp. 2712–2724, 2016.

[12] V. Szebehely, *Theory of Orbits: The Restricted Problem of Three Bodies*. Academic Press, 1967.

[13] P. Gurfil and P. K. Seidelmann, *Celestial Mechanics and Astrodynamics: Theory and Practice*. Springer-Verlag, 2016.

[14] K. C. Howell, "Solar sail orbit operations at asteroids," *Journal of Astronautical Sciences*, vol. 49, pp. 107–125, 2001.

[15] B. K. Shivamoggi, *Nonlinear Dynamics and Chaotic Phenomena: An Introduction*. Springer Science and Business Media, 2014.

[16] D. J. Dichmann, E. J. Doesdel, and R. C. Paffenroth, "The computation of periodic solutions of the 3-body problem using the numerical continuation software AUTO," in *International Conference on Libration Point Orbits and Applications*, vol. 10-14 June 2002, 2002.

[17] M. W.Busch, S. J.Ostro, L. A.M.Benner, M. Brozovic, J. D.Giorgini, J. S.Jao, D. J.Scheeres, C. Magri, M. C.Nolan, E. S.Howell, P. A.Taylor, J.-L. Margot, and W. Brisken, "Radar observations and the shape of near-earth asteroid 2008 ev5," *Icarus*, vol. 212, pp. 649–660, 2011.

[18] T. Gehrels, *Asteroids*. University of Arizona Press, 1979.

[19] G. A. Krasinsky, E. V. Pitjeva, M. V. Vasilyev, , and E. I. Yagudina, "Hidden mass in the asteroid belt," *Icarus*, vol. 158, pp. 98–105, 2002.

[20] A. Borffrafe, J. Heiligers, M. Ceriotti, and C. R. McInnes, "Optical control of solar sails using distributed reflectivity," in *Spacecraft Structures Conference*, 2014.

[21] A. G. de Corral, "Attitude control of a solar sail with variable reflectivity matrix," 2017.

[22] C. R. McInnes, *Solar Sailing: Technology, Dynamics, and Mission Applications*. Springer-Praxis Books, 1999.

[23] G. May-Wilson, "Can a large solar sail be used instead of a small one," 2017.

[24] W. S. Koon, M. W. Lo, J. E. Marsden, and S. D. Ross, *Dynamical Systems, the Three-Body Problem and Space Mission Design*. Springer-Verlag New York Inc, 2011.